

FORMATION OF THE GREEN STABLE α -MnS WITH METASTABLE γ -MnS NANOPARTICLES AND THIN FILMS BY HOMOGENEOUS PRECIPITATION ROUTE

T. XABA^{a,*}, M. AL-SHAKBAN^b

^a*Department of Chemistry, Vaal University of Technology, P/Bag X021, Vanderbijlpark, South Africa*

^b*Department of Physics, College of Science, University of Misan, Iraq*

MnS nanoparticles and thin films were prepared via homogeneous precipitation technique and the films were deposited on glass substrates. Polyvinyl pyrrolidone and polyethylene glycol were used as capping agents. The optical properties showed blue shift when the capping agents were introduced into the nanoparticles. The band gap energies of nanoparticles and thin films were calculated from Tauc's relationship and were found to be between 3.84-4.29 eV which was greater than the band gap of the bulk material. The XRD patterns of the synthesized MnS nanoparticles and thin film possess both cubic and hexagonal structures with lattice parameters $a=b=c=5.2 \text{ \AA}$ for cubic phase and $a=b=3.9 \text{ \AA}$ and $c=6.4 \text{ \AA}$ for hexagonal phase which were close to the reported values. The crystallite sizes were determined using the Scherrer's formula. The SEM images of MnS thin films clearly showed tree-like structures particles with round shaped granules.

(Received April 17, 2020; Accepted August 14, 2020)

Keywords: Manganese sulfide nanoparticles, Thin films, PVP, PEG, UV-Vis, PL, XRD, TEM, SEM

1. Introduction

Thiourea and its derivatives have been widely studied and claimed to be valuable in many applications as pharmaceutical agents, anticancer properties, drug deliveries, antitubercular etc [1]. Semiconductor materials have attracted great interest in many applications due to their morphological structures, sizes, and crystal structures [2]. Metal chalcogenides have gained great interest due to their physical properties and electronic properties in numerous applications such as thermoelectric devices, solar and fuel cells, light-emitting diodes, and semiconductor photocatalysts [3-4]. Manganese sulfide in particular is an important magnetic semiconductor that has displayed considerable applications in many fields such as magnetic semiconductors, photochemical materials, and optoelectronic devices [5]. It is a p-type semiconductor material which exists in three crystalline phases which are the stable cubic rock-salt structure which is a green-colored α -MnS, the pink metastable zinc blende structure of β -MnS, and the wurtzite structure of γ -MnS [6]. The preservation of particle size, shape and crystallography during the synthesis of nanoparticles is of strictly importance. Capping molecules are normally used during the synthesis of nanomaterials to keep them into their original form. Various methods for the synthesis of MnS nanoparticles and thin films have been reported. Lately, these approaches include chemical bath deposition, hydrothermal, solvothermal, spray produced, molecular beam epitaxy and microwave irradiation [7].

Jiang *et al.* [8] reported the shape-controlled synthesis and properties of manganese sulfide materials through biomolecule-assisted hydrothermal process. Soluble hydrated manganese chloride was used as a metal source and L-cysteine was used as precipitator and a complexing reagent. The sea urchin-like γ -MnS and octahedron-like α -MnS microcrystals were obtained by adjusting reaction time and hydrothermal temperature. As far as we know, there is no study based on the preparation of MnS nanoparticles and thin films using homogeneous precipitation method that had been reported in the past. In the present work, we report the synthesis of manganese

* Corresponding author: thokozanix@vut.ac.za

sulfide nanoparticles and thin films via homogeneous precipitation approach which is a chemical method that is relatively inexpensive, very simple, non-toxic, and less time consuming. The effect of capping agent was examined with polyvinyl pyrrolidone (PVP) and polyethylene glycol (PEG) and the optical properties together with morphological studies were analyzed with UV-Vis, PL, XRD, TEM and SEM.

2. Experimental

2.1. Materials

Pyrrolidone, thiourea, 1-methyl thiourea, manganese acetate dihydrate 99%, 1 M ammonium hydroxide, polyvinyl pyrrolidone, polyethylene glycol, methanol, and acetone were reagents from Sigma-Aldrich and were all used without further purification. The glass microscope slides were purchased from Thermo Fisher Scientific.

2.1.1. Preparation of the ligands

(Z)-2-(pyrrolidin-2-ylidene)thiourea (**L1**) and (Z)-2-(pyrrolidin-2-ylidene)-1-methylthiourea (**L2**) ligands were prepared according to the reported procedure [9-10]. In a typical experiment, pyrrolidone or 1-methyl-2-pyrrolidone (1 mmol) in hot methanolic (20 mL) was mixed with (20 mL) hot methanolic solution of thiourea (1 mmol). The mixture was refluxed for 2hrs on the water bath at 70 °C as shown in Scheme 1. The white crystals were then filtered, washed with acetone and dried in a desiccator.

2.1.2. Synthesis of the MnS nanoparticles and thin films

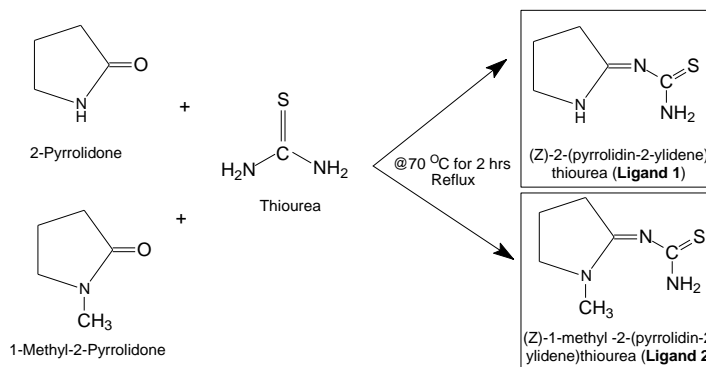
The synthetic procedure for the preparation of MnS nanoparticles and thin films was done by combining a warm 50% methanol (20 mL) solution of manganese acetate dihydrate (5 mmol) with (20 mL) warm 50% methanolic solution of the **L1** or **L2** (10 mmol). The mixture was then transferred into a 100 mL two necked flask with two parallel glass substrates which was inserted at the other end of the flask to ensure the proper deposition of the particles onto slides. The reaction was refluxed for 1hr in a water bath at 70 °C which was supported by the stirrer. The glass substrates were then removed from the reaction chamber, dried and reserved for further analysis. The capping process was achieved by transferring the MnS nanoparticles into 1% PVP or PEG solution which was adjusted to a higher pH with ammonium hydroxide solution. The MnS nanoparticles were separated from the solution using centrifuge technique, washed three times with methanol, dried and analyzed.

2.2. Characterisation

UV-1800 Shimadzu spectrophotometer and Gilden Fluorescence were used to investigate the optical properties of MnS nanoparticles and thin films by dissolving the nanoparticles in distilled water using a quartz cuvette with 1 cm path length. Phillips X'Pert diffractometer was used to obtain XRD patterns of the nanoparticles and films using a secondary monochromated Cu K α radiation ($\lambda = 1.54060\text{\AA}$) at 40 Kv/30mA. The analysis was done from a glancing angle of incidence detector over 10 to 80° 2 θ values in steps of 0.0167 with a scan speed of 0.0452. Tecnai F30 FEG TEM instrument was used to collect the images of the MnS nanoparticles at an accelerating voltage of 300Kv and Philips XL 30FEG SEM instrument was used to collect the micrograms of the thin films.

3. Results and discussion

The substituted thiourea ligands, (Z)-2-(pyrrolidin-2-ylidene)thiourea (**L1**) and (Z)-2-(pyrrolidin-2-ylidene)-1-methylthiourea (**L2**) were prepared as show in Scheme 1 and used to synthesize manganese sulfide nanoparticles and thin films through modified homogeneous precipitation route.



Scheme 1. Preparation of (Z)-2-(pyrrolidin-2-ylidene) thiourea (L1) and (Z)-2-(pyrrolidin-2-ylidene)-1-methyl thiourea (L2) ligands.

3.1. Optical properties

The optical absorption of the synthesized MnS nanoparticles and their corresponding thin films are shown in Fig. 1. The obtained absorption spectra in Fig. 1(a) clearly indicate that the synthesized MnS nanoparticles from **L1** have absorption in the visible range with sharp absorption band edges at 349, 319 and 344 nm. The spectra of the capped nanoparticles were blue shifted compared to the uncapped MnS nanoparticles. Fig. 1(c) shows the absorption spectra of the MnS thin films (prepared from **L1** and **L2**) with band edges at 352 and 368 nm. The band gap energies were calculated using Tauc's relationship [11]. Fig. 1(b)&(d) show band gap energies (E_g) of nanoparticles and thin films at 3.84, 4.29, 4.28, 4.02 and 4.00 eV that were higher compared to the direct band gap value of the MnS bulk material which is 3.70 eV [12]. This increase in band gap values can be ascribed to quantum confinement effect.

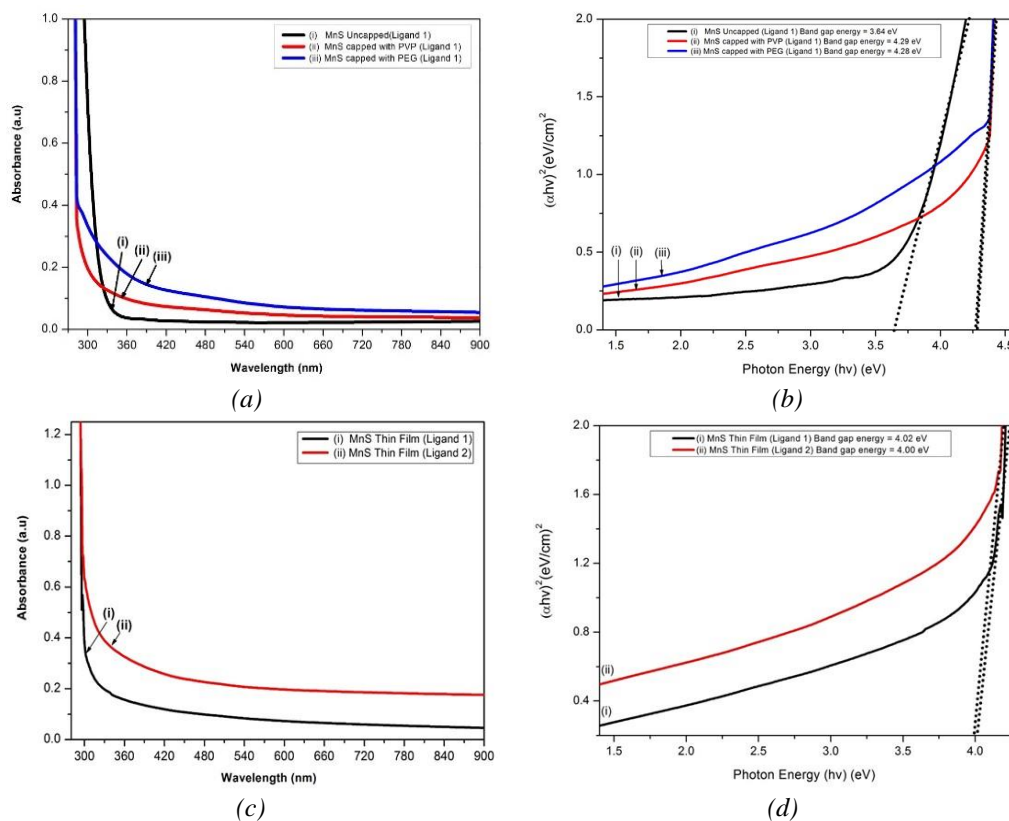


Fig. 1. Absorption spectra (a) & (c), Tauc plots (b) & (d) of the uncapped (i) PVP (ii) & PEG (iii) capped MnS nanoparticles and thin films.

Emission spectra of the synthesized nanoparticles and thin films are shown in Fig.2(a)&(b). The spectra of the MnS nanoparticles capped with PVP and PEG in Fig.2(a) show the emission maxima at 440 and 441 nm which are blue shifted compared to the uncapped nanoparticles at 450 nm. Fig.2(b) reveals the emission spectra of the MnS thin films prepared from two ligands with the emission peaks at 456 and 470 nm.

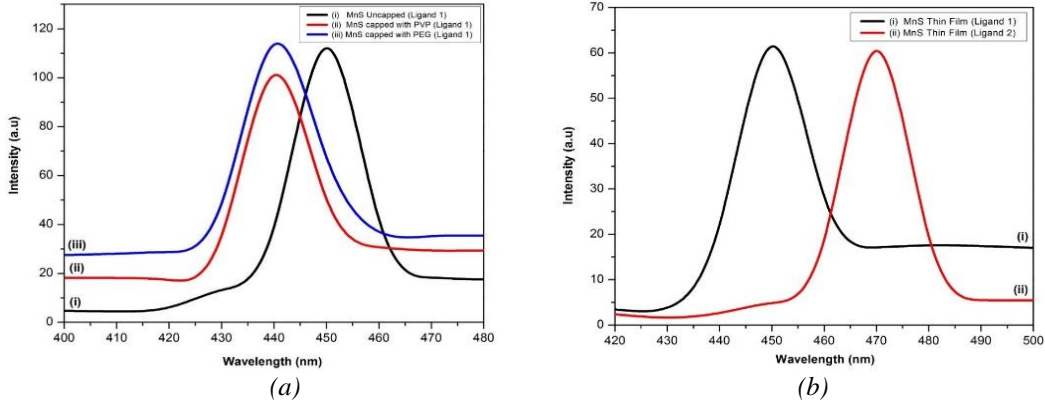


Fig. 2. Photoluminescence spectra of the uncapped (i) PVP (ii) & PEG (iii) capped MnS nanoparticles (a) and thin films (b).

3.2. Structural properties

XRD patterns of MnS nanoparticle and films are represented in Fig. 3(a)&(b). All the patterns showed a mixture of two phases that can be indexed to cubic α -MnS with lattice constants of $a = b = c = 5.2 \text{ \AA}$ (JCPDS, File No.65-6745) and hexagonal wurzite γ -MnS with lattice constants of $a = b = 3.9 \text{ \AA}$ and $c = 6.4 \text{ \AA}$ (JCPDS, File No.40-1289) which were very closed to the previously reported results [13-14]. The diffraction peaks of the capped MnS nanoparticles in Fig.3(a) located at about 19° may be attributed to PVP and PEG [15]. It was also noted that some of the peaks from these diffraction patterns were hidden due to the presence of the capping agent. The diffraction peaks were very broad which is an indication of nanosize particles. The average crystallite sizes were estimated from Scherrer's formula [16]:

$$D = \frac{0.9 (\lambda)}{\beta \cos \theta} \quad (1)$$

where D is crystallite size, λ is wavelength (1.5418 \AA), β is full width half maximum (FWHM) and θ is the Bragg's angle corresponding peak. The calculated crystallite size of the uncapped MnS nanoparticles was found to be 7.35 nm whereas for the capped nanoparticles was 2.83 nm.

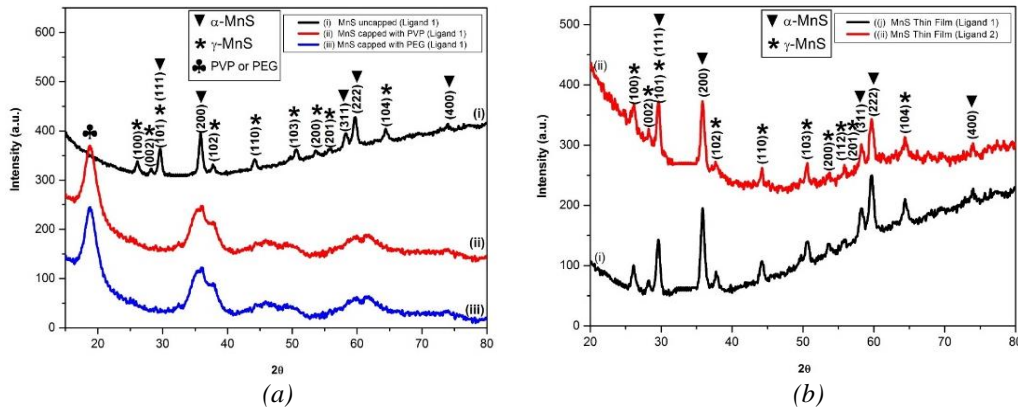


Fig. 3. X-ray diffraction patterns of the uncapped (i) PVP (ii) & PEG (iii) capped MnS nanoparticles (a) and thin films (b).

The morphology of the synthesized MnS nanoparticles and thin films were revealed by TEM and SEM instruments as shown in Fig. 4. The TEM images in Fig. 4(a)&(b) display few spherical shaped particles that were covered by petal-like structures and nano-sheets for PVP and PEG capped MnS nanoparticles which is similar to the reported results [17]. SEM was used to study the surface morphology of the deposited MnS films on the glass substrate. Fig. 4(c)&(d) reveals the SEM micrograms of the prepared thin films. Fig. 4(c) micrographs clearly composed of tree-like structures particles with round shaped granules that appear to be quite uniform and analogous to each other with the particle sizes of $0.424\pm 0.094\ \mu\text{m}$. Fig. 4(d) also projects the elongated branch tree-like structures that are connected to each other.

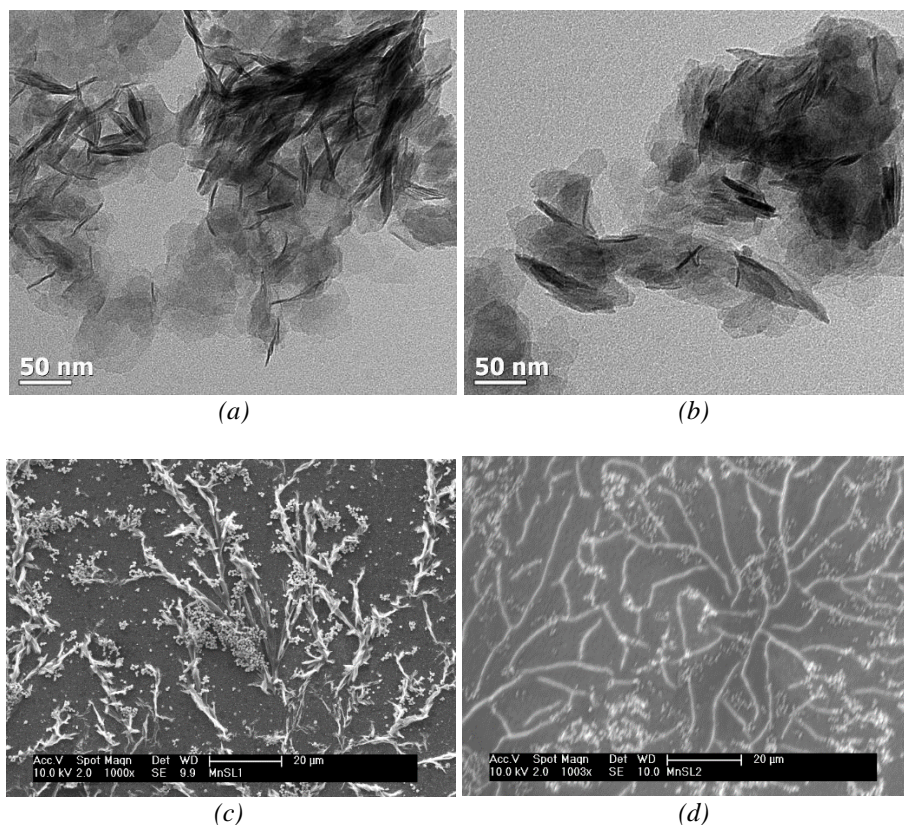


Fig. 4. TEM images of the PVP (a) & PEG (b) capped MnS nanoparticles and SEM micrograms of the MnS thin films prepared from L1 (c) & L2 (d).

4. Conclusions

Manganese sulfide nanoparticles and thin films have been successfully synthesized by homogeneous precipitation route. The absorption and photoluminescence studies showed the blue shift on the capped MnS nanoparticle compared to the uncapped nanoparticles. The MnS thin films that were prepared from **L2** displayed a red shift compared to the thin films that was synthesized with **L1**. The XRD patterns of the synthesized MnS nanomaterials and films yielded stable α -MnS and metastable γ -MnS crystallites. The crystallite sizes determined from XRD using Scherrer's equation were found to be 2.83 nm and 7.35 nm for the capped and uncapped MnS nanoparticles, respectively. It is clear from this study that the capping molecules have a great impact on the formation of the nanomaterials.

Acknowledgements

The authors would like to acknowledge the University of Manchester for providing necessary facilities, National Research Foundation (NRF) (Thuthuka Grant Holder no: TTK170508230117), and Vaal University of Technology for the funding.

References

- [1] A. O. Celen, B. Kaymakcioglu, S. Gumru, H. Z. Toklu, F. Aricioglu, *Marmara Pharm J.* **15**, 43 (2011).
- [2] J. Zhang, R. Shi, C. Zhang, L. Li, J. Mei, S. Liu, *J. Mater. Res.* **33**, 4224 (2018).
- [3] X. Li, J. Yu, M. Jaroniec, Hierarchical photocatalysts. *Chem. Soc. Rev.* **45**, 2603 (2016).
- [4] M. Meikandan, M. Karthick, M. Sundarraj, B.R. Aravindra, *Chalcogenide Letters* **16**, 405 (2019).
- [5] Y. Zheng, Y. Cheng, Y. Wang, L. Zhou, F. Bao, C. Jia, *J. Phys. Chem. B* **110**, 8284 (2006).
- [6] D. B. Fan, H. Wang, Y. C. Zhang, H. Cheng, B. Wang, H. Yan, *Mater. Chem. Phys.* **80**, 44 (2003).
- [7] L. Amirav, E. Lifshitz, *J. Phys. Chem. B* **110**, 20922 (2006).
- [8] J. Jiang, R. Yua, J. Zhua, R. Yia, G. Qiu, Y. Heb, X. Liu, *Materials Chemistry and Physics* **115**, 502 (2009).
- [9] T. Xaba, M. J. Moloto, N. Moloto, *Materials Letters* **146**, 91 (2015).
- [10] T. Xaba, J. Magagula, O. B. Nchoe, *Materials Letters* **229**, 331 (2018).
- [11] J. Tauc, R. Grigorovici, A. Vancu, *Phys. Status Solidi* **15**, 627 (1966).
- [12] C. D. Lokhande, A. Ennaoui, P. S. Patil, M. Giersig, M. Muller, K. Diesner, H. Tributsch, *Thin Solid Films* **330**, 70 (1998).
- [13] S. H. Chaki, S.M. Chauhan, J.P. Tailor, M.P. Deshpande, *J. Mater Res. Technol.* **6**, 123 (2017).
- [14] J. Lu, P. Qi, Y. Peng, Z. Meng, Z. Yang, W. Yu, Y. Qian, *Chem. Mater* **13**, 2169 (2001).
- [15] A. Abedini, E. Saion, F. Larki, A. Zakaria, M. Noroozi, N. Soltani, *Int. J. Sci.* **13**, 11941 (2012).
- [16] S. K. Panda, A. Antonakos, E. Liarokapis, S. Bhattacharya, S. Chaudhuri, *Mater Res Bull.* **42**, 576 (2007).
- [17] M. Villalobos, B. Lanson, A. Manceau, B. Toner, G. Sposito, *American Mineralogist* **91**, 489 (2006).